

Novel Approach in Investigation of the Poly(Acrylic Acid) Hydrogel Swelling Kinetics in Water

B. Adnadjevic, J. Jovanovic

Faculty of Physical Chemistry, Studentski trg 12-16, 11000 Belgrade, Serbia

Received 3 March 2006; accepted 26 August 2007

DOI 10.1002/app.27451

Published online 5 December 2007 in Wiley InterScience (www.interscience.wiley.com).

ABSTRACT: The swelling kinetics curves of structurally defined poly(acrylic acid) hydrogel in bidistilled water at temperatures: 25, 30, 35, 40, and 45°C were determined. The possibility of kinetically explaining the isothermal swelling process by applying the following models: reaction controlled by diffusion, first order chemical reaction kinetics, and second order chemical reaction kinetics, was investigated. It was found that kinetically explaining the swelling process using these methods was limited to only certain parts of the process. The swelling process in bidistilled water was described in full range assuming that the

hydrogel's swelling rate was a kinetically controlled reaction by the rate of the movement of reactive interface of hydrogel. Based on that model, the kinetic parameters, activation energy (E_a) and preexponential factor (A), of the swelling process were determined to be $E_a = 35$ kJ/mol and $\ln A = 8.6$. A possible mechanism of the investigated swelling process was discussed. © 2007 Wiley Periodicals, Inc. *J Appl Polym Sci* 107: 3579–3587, 2008

Key words: activation energy; hydrogels; kinetics parameters; modeling; poly(acrylic acid); swelling; swelling kinetics

INTRODUCTION

Hydrogels are three-dimensional crosslinked polymeric structures that are able to swell in an aqueous environment. Because of its characteristic properties such as swellability in water, hydrophilicity, and also very often good biocompatibility, hydrogels have been utilized in a wide range of biological, medical, pharmaceutical, and environmental applications.^{1,2} Hydrogels of acrylic polymers and their copolymers have been reported as hydrogels with adjustable swelling kinetics that display special properties.³ It has also been reported that the presence of polyacrylic segments in hydrogels significantly increases their ability to uptake water.⁴ It is predictable that, due to the presence of carboxylic acid side groups, the swelling behavior of poly(acrylic acid) (PAA) hydrogels is highly dependent on the pH of the surrounding medium.⁵

The application of hydrogels could be affected significantly by their swelling properties. There are various examples of different kinetics of the swelling processes for various hydrogels. The kinetics of swelling of hydrogels are most frequently formally

described as processes controlled by diffusion or as first order chemical reactions.⁶ The swelling of poly(acrylamide)/poly(mono-*n*-alkyl itaconates) hydrogels at different pH values at 25°C has been investigated and the results indicated that the investigated swelling processes followed second-order kinetics.⁷ Studies on the swelling of acrylamide/crotonic acid hydrogels in distilled water at 25°C have been undertaken and it was found that they followed non-Fickian diffusion.⁸ Karadağ et al. investigated the dynamics and equilibrium swelling behavior of radiation-induced acrylamide/itaconic acid hydrogels in water at 25°C. The diffusion type of these hydrogels was found to be non-Fickian.⁹ The swelling behavior of acrylic acid hydrogels synthesized by γ -radiation crosslinking of poly(acrylic acid) was investigated by allowing them to swell in a buffered media of pH 4 and pH 7. It was found that the swelling mechanism depended on the pH of the swelling medium and the concentration of PAA during irradiation.¹⁰

In the present study, the isothermal kinetics of the swelling of PAA hydrogel in bidistilled water at a temperature range from 25 to 45°C was determined experimentally and it was examined theoretically using both traditional and newly established methods. The aim of this work was to investigate the kinetics of swelling and to determine the kinetic parameters (activation energy and preexponential factor) for swelling in bidistilled water of the synthesized and structurally defined poly(acrylic acid) hydrogel sample.

Correspondence to: J. Jovanovic (jelenajov2000@yahoo.com or jelenaj@ffh.bg.ac.yu).

Contract grant sponsor: Ministry of Science and Environmental Protection of Serbia by project 142025G.

EXPERIMENTAL

Materials

Acrylic acid (AA) monomer in glacial form, was obtained from Merck-Darmstadt, Germany. The initiator, sodium persulfate ($\text{Na}_2\text{S}_2\text{O}_8$) and sodium thiosulfate ($\text{Na}_2\text{S}_2\text{O}_5$), both p.a. purity were also supplied by Merck and were used as a redox initiator pair with hydrogen peroxide (H_2O_2 , 30%), obtained from Zorka-Sabac, Serbia, and Montenegro. *N,N'*-methylenebisacrylamide (NMBA), purchased from Merck Darmstadt, Germany, was used as a crosslinking agent. Ethylenediaminetetraacetic acid (EDTA), p.a., was also purchased from Merck Darmstadt, Germany. Sodium carbonate (Na_2CO_3), p.a., Zorka-Sabac, Serbia, and Montenegro, was used for neutralization. All chemicals were used as received. Bidistilled water was used in the polymerizations and swelling studies.

Synthesis of poly(acrylic acid) hydrogel

The poly(acrylic acid) hydrogel that has been used in this investigation was synthesized following the procedure based on the simultaneous radical polymerization of AA and crosslinking the formed poly(acrylic acid) according to following procedure:¹¹

Hydrogel synthesis was performed in a polymerization reactor in a nitrogen atmosphere equipped with a magnetic stirrer, reflux condenser, nitrogen inlet, and a thermometer. A monomer solution was prepared from: 80 mL of melted glacial AA dissolved in 180 mL of distilled water, and 0.8 g of NMBA, and 0.08 g of EDTA both dissolved in 60 mL of distilled water. This monomer solution was placed in the reactor, stirred, and deoxygenated with nitrogen gas bubbling through the solution for 60 min. The initiator stock solutions were: sodium persulfate, sodium thiosulfate (2.5 g of each were dissolved in 22.5-mL bidistilled water), and hydrogen peroxide, 30%. When the deoxygenation time finished, the initiator solutions were added to the following monomer solutions: 2.4 mL of sodium persulfate solution, 10 mL of hydrogen peroxide, and 1.2 mL of sodium thiosulfate solution. The reaction mixture was then slightly gradually warmed up to 50°C until there was a dramatic increase in the reaction mixture's temperature (gel-point) and then it was left following 4 hours at 80°C. The obtained gel-type product was converted into the Na^+ form (60%) by neutralizing it with a 3% solution of Na_2CO_3 . The resulting hydrogel was cut to approximately equal discs and placed in excess distilled water. The water was changed seven times every 5 h (or 12 h during the night), to remove the unreacted monomers and the sol fraction of the polymer. The obtained hydrogel was then dried in an air oven in a

temperature regime of 80°C for 2 h, 90°C for 3 h, and 105°C until the solid reached constant mass. The obtained products were stored in a vacuum exicator before use.

Xerogel physicochemical characterization

The xerogel was characterized by the following structural properties: xerogel density (ρ_{xg}), crosslink density (ρ_c), distance between macromolecular chains (d), as well as by X-ray diffraction and scanning electron microscopy analyses.

Xerogel density (ρ_{xg}) determination

The apparent density of the synthesized sample was determined according to a procedure described in the literature, using *n*-hexane as the nonsolvent.¹²

The crosslink density (ρ_c) and the distance between the macromolecular chains (d) were calculated according to methods proposed by Gudeman and Peppas,¹³ using the following equations:

$$\rho_c = \frac{\rho_{\text{xg}}}{M_c} \quad (1)$$

$$d = 0.154 \cdot v_2^{1/3} [0.19 \cdot M_c]^{1/2} \quad (2)$$

where M_c is the molar mass between the network crosslinks which is a nominal value estimated from initial composition:

$$M_c = \frac{72}{2X} \quad (3)$$

where X is nominal crosslinking ratio and v_2 is the polymer gel volume fraction in the equilibrium swollen state at 25°C, and which was determined as follows [eq. (4)]:

$$v_2 = \frac{V_p}{V_{g,s}} \quad (4)$$

where V_p is the volume of the dry polymer sample and $V_{g,s}$ is the gel sample volume after equilibrium swelling:

$$V_{g,s} = \frac{W_{a,s} - W_{h,s}}{\rho_h} \quad (5)$$

where $W_{a,s}$ is the weights of polymers after swelling in air, $W_{h,s}$ is the weights of polymers after swelling in *n*-hexane and ρ_h density of *n*-hexane.

Swelling experiments

The swelling parameters were determined by leaving dried hydrogels (xerogels) with an average weight of

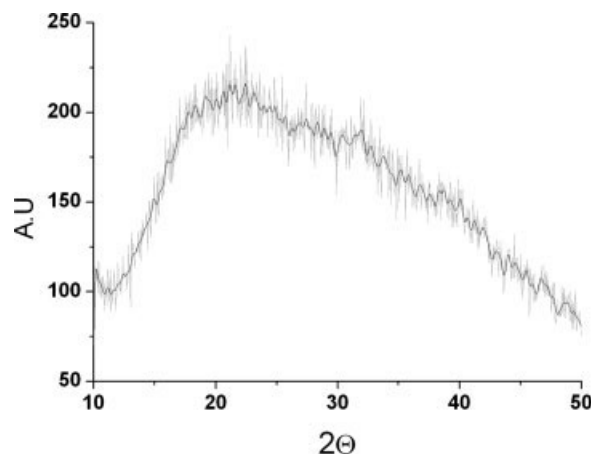


Figure 1 X-ray diffraction of the investigated xerogel.

0.1 g ($\pm 5\%$) to swell in distilled water at temperatures ranging from 25 to 45°C. At the beginning of each experiment, a sample of xerogel was measured by weight and then it was immersed to swell in excess water. At predetermined time intervals the swollen gel was removed from the water and weighed. This was done until the hydrogel reached equilibrium and obtained a constant mass. Since the swollen gel appeared to be fragile, they were put on a grid boat with a mesh size of 1 mm. This technique allowed hydrogel to be gently placed in water and to be weighed without breaking it. Each time the grid boat with the polymer was removed from water, it was gently dried with paper tissue to remove adhering water.

Determination of the swelling degree

The isothermal swelling degree (SD), defined as the difference between the weight of the swollen hydrogel sample at time (t) (m_t) and the weight of dry hydrogel (xerogel) sample (m_o) divided by the weight of the dry sample (m_o), was calculated according to eq. (6) and determined as a function of time:

$$SD[\%] = \frac{m_t - m_o}{m_o} \cdot 100 \quad (6)$$

The equilibrium swelling degree (SD_{eq}) is the SD of the swollen hydrogel at equilibrium, i.e., the hydrogel sample which attained a constant mass (m_{eq}). For each sample at least three swelling measurements were performed and the average values were reported.

Normalized swelling degree

The normalized SD (α) was defined as the ratio between the SD at time (t) and the equilibrium SD (SD_{eq}):

$$\alpha = \frac{SD}{SD_{eq}} \quad (7)$$

Apparatus

X-ray diffraction

X-ray diffraction (XRD) analysis of the investigated xerogel were performed using a Philips PW 1050 diffractometer with a monochromated Cu $K\alpha$ radiation ($P = 1.5407\text{\AA}$) and an automatic divergence slit. A scan speed of 0.040° 2R/s and a recording speed of 10 mm/°2θ was used.

Scanning electron microscopy

The microstructure of the xerogel surface was observed by a scanning electron microscopy (SEM) using a JEOL 5300 instrument. After coating the xerogel samples with gold, they were mounted on an aluminum sample mount. All micrographs were the product of secondary electron imaging used for surface morphology identification at different magnifications.

RESULTS AND DISCUSSION

The XRD patterns of the investigated xerogel are presented in Figure 1. One broad complex peak in the range 10–50 2θ degrees, with a maximum at about 22 2θ degrees may be seen in the PAA xerogel diffractogram. This shape observed in the X-ray diffractogram is characteristic of an amorphous polymer structure.

Figure 2 presents an image of the microstructure of the synthesized xerogel surface obtained by SEM at magnifications of (a) 2000 and (b) 3500. It can be clearly observed that the xerogel surface morphology is crinkled, porous, and open with dominant entangled and crosslinked chains.

Based on the obtained results presented in Table I and in Figures 1 and 2, it may be concluded that the synthesized xerogel was an amorphous structure with a medium crosslinking density and macroporous (pore with average diameter $\geq 50\text{nm}$).

Figure 3 shows the swelling isotherms of the synthesized xerogel of crosslinked poly(acrylic acid) in sodium form, in distilled water at different temperatures. As can be seen from the results presented in Figure 3, the swelling isothermal curves are similar by shape at all of the investigated temperatures. Three characteristic shapes of SD change with swelling time may be distinguished in all of the swelling curves: a linear part, a nonlinear part, and a saturation range or plateau.

Table II presents the temperature changes of the equilibrium SD (SD_{eq}), the initial swelling rate (denoted v_{in}) and the so called “range of applicabil-

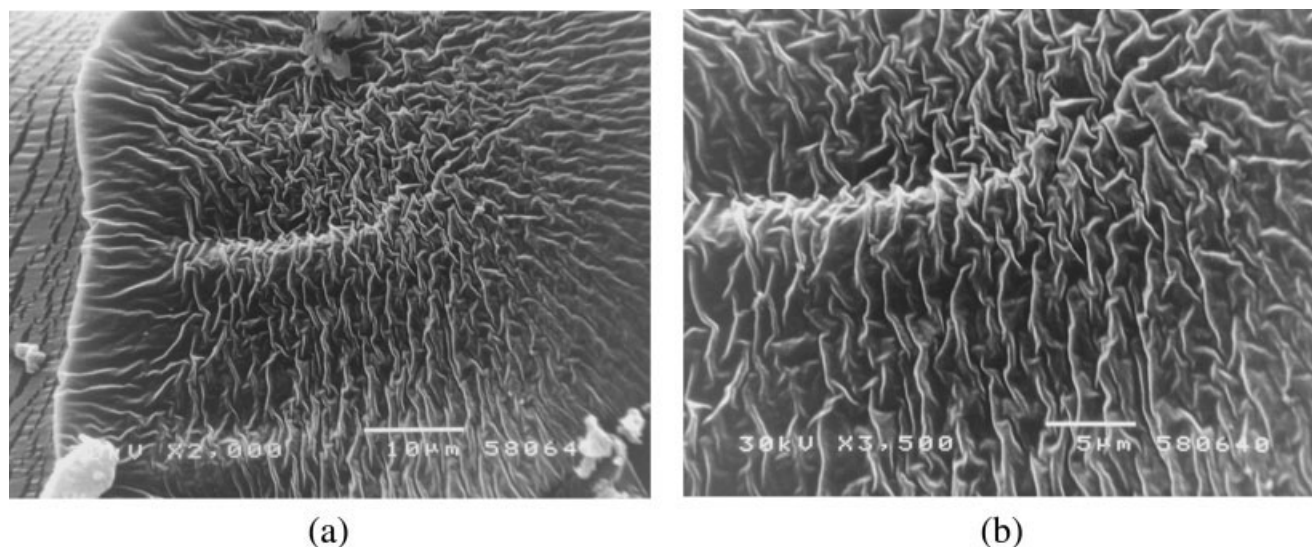


Figure 2 (a) SEM micrograph of the xerogel surface, magnification 2000. (b) SEM micrograph of the xerogel surface, magnification 3500.

ity" (denoted P). The initial swelling rate (v_{in}) is defined as the ratio of the SD at the final point of the linear part of the swelling curve (SD_{in}) to swelling time which corresponds to the linear part of the swelling curve (t_{in}) [eq. (8)].

$$v_{in} = \frac{SD_{in}}{t_{in}} \quad (8)$$

The range of applicability (P) represents a region of the SD, i.e., a normalized SD (α) within which the kinetic curve and the model of the kinetics of swelling is linear.

As the temperature of swelling increases, the swelling equilibrium degree (SD_{eq}) increases as well as the initial swelling rate, while the range of applicability varies with temperature.

When the kinetics of swelling are determined by the rate of diffusion this is known as Case I sorption. The swelling medium permeation is then governed by Fickian laws of diffusion and the SD of a material (SD) obeying these laws is proportional to the square root of time^{6,8}: $SD = k t^{1/2}$.

Figure 4 presents a plot of the SD as a function of the square root of time ($t^{1/2}$) for different swelling temperatures.

TABLE I
Structural Properties of the Synthesized Xerogel

Physico-chemical properties	Value
Xerogel density (ρ_{xg}), (kg/m ³)	1140
Molar mass between the crosslinks, M_c , (g/mol)	8200
Cross-link density (ρ_c), (mol/m ³)	1.39×10^{-4}
Distance between the macromolecular chains (d), (nm)	1.47

The results obtained as a plot of the SD as a function of the square root of time at all the investigated temperatures significantly deviate from straight lines (Fig. 4). The region of very small SDs as well as region of very high SDs especially deviates from straight lines. The dependence of SD on square root of time gives the best fits for the middle stages of the swelling process. Swelling rate constants (k_D) that are calculated from the slopes of curves (SD) versus ($t^{1/2}$) and corresponding values for the range of applicability (P) and correlation coefficients (R) for different temperatures for Fickian type diffusion are given in Table III.

These results imply that the so-called Fickian type of solvent diffusion into the hydrogel has not the dominant influence on the kinetics of the hydrogel's swelling nor on the changes of the swelling kinetics

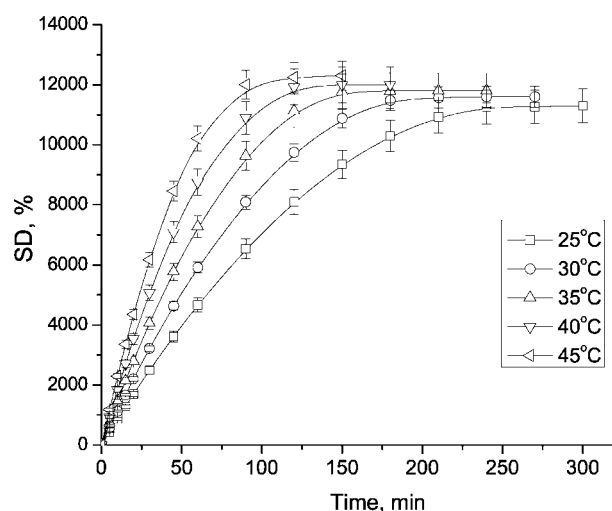


Figure 3 The swelling isotherms of PAA hydrogel in bidistilled water at different temperatures.

TABLE II
Temperature Influence on the Equilibrium Swelling Degree (SD_{eq}), Initial Swelling Rate (v_{in}), and Range of Applicability (P)

Temperature (°C)	SD_{eq} (%)	v_{in} (%/min)	P (%)	t_f (min)	v_f (%/min)
25	11,300	75	0–33	242	46.7
30	11,600	107	0–27.7	210	55.2
35	11,800	135	0–34.5	150	78.7
40	12,000	156	0–32.5	141	85.1
45	12,300	193	0–42.3	120	102.5

with temperature within the investigated temperature range.

When the rate of progress of swelling is determined by the rate of expansion of the material, the amount of absorption is observed to be directly proportional to time which is known as Case II sorption. The isothermal kinetics of the swelling could be described with first order kinetics reaction and the following equation [eq. (9)] can be applied:^{6,7}

$$\ln \frac{SD_{eq}}{SD_{eq} - SD} = k \cdot t \quad (9)$$

i.e., the plots of $\ln \frac{SD_{eq}}{SD_{eq} - SD}$ versus time (t) give straight lines.

Figure 5 presents the dependence of $\ln \frac{SD_{eq}}{SD_{eq} - SD}$ on time for the investigated hydrogel swelling at investigated temperatures.

The plots of $\ln \frac{SD_{eq}}{SD_{eq} - SD}$ as a function of time (t) as a function of time (t) give straight lines only at the beginning of the swelling process until a limited extent of the process, that are the range of applicability (P). The temperature changes of P for first-order kinetics, the corresponding values for correlation coefficients (R), and the swelling rate constants (k) calculated from the slopes of curves (Fig. 5) are presented in Table IV.

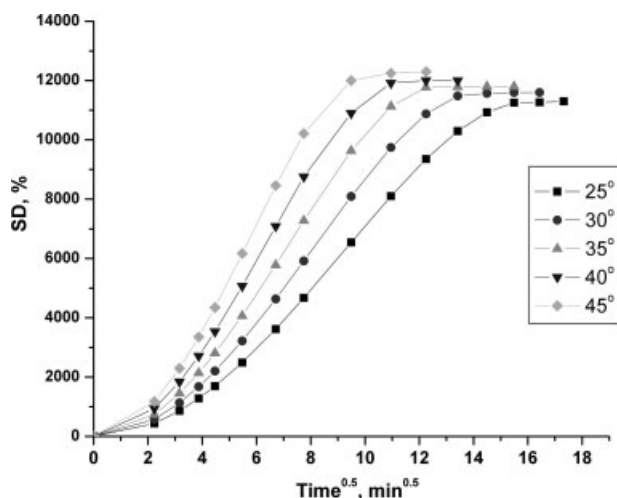


Figure 4 The plot of SD as a function of the square root of time at investigated temperatures.

TABLE III
Temperature Changes of Ranges of Applicability (P), Swelling Rate Constants (k) and Correlation Coefficients (R) for Fickian Type of Diffusion

Temperature (°C)	P (%)	R	k_D ($\text{min}^{-1/2}$)
25	22–82.8	0.9997	1028
30	27.7–84	0.9998	1202
35	23.8–82	0.9998	1371
40	22.56–73	0.9996	1571
45	27.2–83	0.9999	1788

As swelling temperature increases swelling rate constants also increase while their range of applicability decrease. When isothermal kinetics of swelling could be described by the model of second order chemical kinetics reaction [eq. (10)], a plot t/SD versus time gives straight lines.

$$\frac{t}{SD} = kt + B \quad (10)$$

where $B = \frac{1}{SD_{eq}}$.

Figure 6 presents a plot of t/SD versus time for the investigated hydrogel swelling at investigated temperatures.

The dependence of t/SD on time (t) gives straight lines only in the last stages of the swelling process, i.e., for very high values of SD . Table V presents temperature changes of range of applicability for second-order kinetics and swelling rate constants calculated from the slopes of curves. From the obtained results it is obvious that the calculated constants do not show any regular changes with temperature, thus they cannot be considered relevant for the investigated swelling process.

According to the obtained results, the isothermal kinetics of swelling of the PAA hydrogel in water may be described by the actually known kinetics models only at limited intervals of the swelling pro-

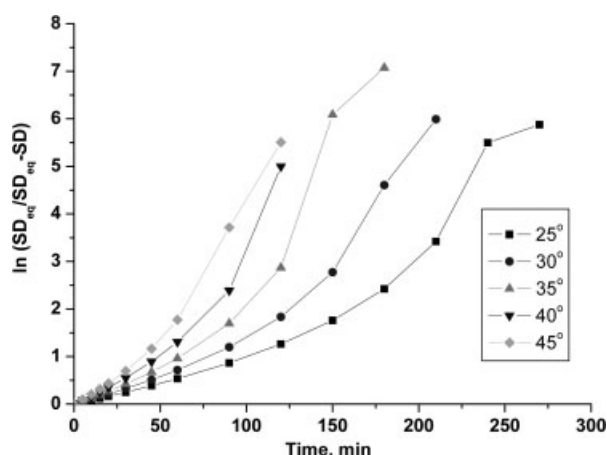


Figure 5 The plot of $\ln \frac{SD_{eq}}{SD_{eq} - SD}$ versus time at investigated temperatures.

TABLE IV
Temperature Changes of Ranges of Applicability (P), Swelling Rate Constants (k) and Correlation Coefficients (R) for First-Order Kinetics

Temperature (°C)	P (%)	R	k (min ⁻¹)
25	0–71.7	0.996	0.01031
30	0–69.8	0.996	0.01308
35	0–61.7	0.998	0.01589
40	0–59.0	0.998	0.01979
45	0–50.1	0.998	0.02317

TABLE V
Temperature Changes of Ranges of Applicability (P), Swelling Rate Constants (k) and Correlation Coefficients (R) for Second-Order Kinetics

Temperature (°C)	P (%)	R	k 10 ⁵ (% ⁻¹)
25	91.11–100	0.9995	7.6272
30	93.75–100	0.9984	7.9937
35	94.32–100	0.9989	8.0574
40	90.83–100	0.9974	7.5538
45	83.02–100	0.996	7.08504

cess, thus we tried to investigate the possibility of applying one new method to the kinetics of swelling. This method which is the so-called “model of reduced time” is widely used to analyze the reaction models of solid state reactions.¹⁴

According to the procedure, the kinetic model of the swelling process was determined by comparing (graphically and analytically) the experimentally obtained function for the investigated process: $\alpha_e = f(t_N)$, with the curves of the theoretical functions $\alpha = f(t_N)$, for different solid state reaction models¹⁵ where α is the normalized SD [eq. (7)] and t_N is the so-called reduced time:

$$t_N = \frac{t}{t_{0.9}} \quad (11)$$

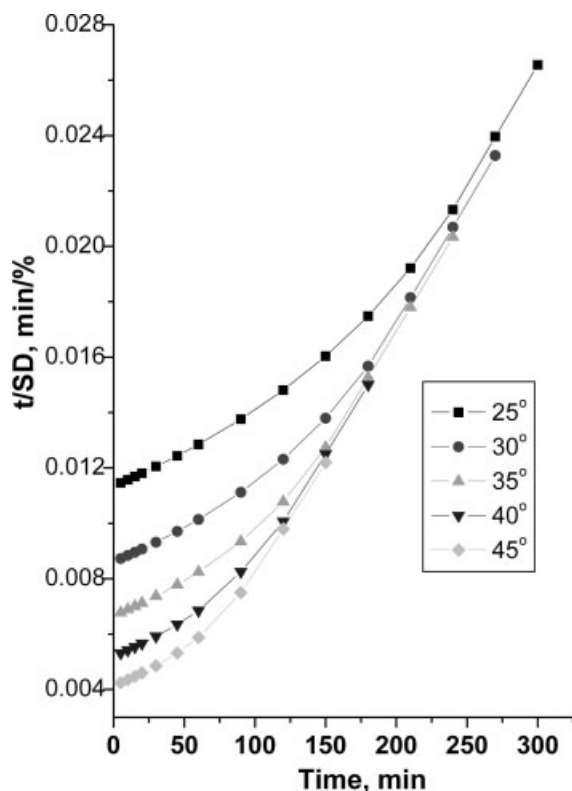


Figure 6 The plot of t/SD versus time at investigated temperatures.

where $t_{0.9}$ is the interaction time at $\alpha = 0.9$.

The sets of common kinetics reaction models that are used to analyze the investigated swelling kinetics models are presented in Table VI.^{15,16}

Figure 7 shows the plot of $\alpha = f(t_N)$ for theoretical reaction models given in Table VI (solid curves) and the experimental plots $\alpha = f(t_N)$ for the swelling of the used poly(acrylic acid) hydrogel in distilled water (\square).

Based on the results presented in Figure 7, it may be concluded that the kinetics of isothermal swelling of PAA hydrogel in distilled water could be described with the kinetics model “R2” which is a “phase boundary controlled reaction, i.e., contracting area reaction” (refer to Table VI).¹⁷ That would imply that the following expression should be valid:

$$1 - (1 - \alpha)^{1/2} = k_m t \quad (12)$$

where k_m is the model’s constant rate.

Figure 8 presents the dependence of $1 - (1 - \alpha)^{1/2}$ on time at different investigated temperatures, for PAA swelling in distilled water. For a very wide range of applicability ($P \geq 90\%$) at all of the investigated temperatures, the dependence $[1 - (1 - \alpha)^{1/2}]$ on time gave straight lines.

The model’s swelling rates constants (k_m) were determined based on the slopes of the lines that were obtained from eq. (12) and presented in Figure 8 are shown in Table VII.

Based on the obtained results presented in Table VII, it is easy to observe that as the temperature of swelling increases the model’s swelling rates constants (k_m) increase as well. Because the determined rate constants increase exponentially with temperature increase, it was possible to determine the kinetics’ parameters (E_a and $\ln A$) by applying the well-known Arrhenius equation.

The Arrhenius plots of $\ln k$ from $(1/T)$ for all examined kinetics models are presented in Figure 9. As it can be easily seen from the presented plots, the excellent correlations for the dependence of $\ln k$ on inverse temperature $(1/T)$ for all applied models are obtained.

Table VIII presents summarized results of the kinetics’ parameters (E_a and A) determined from var-

TABLE VI
The Set of Kinetics Models used to Determine the Kinetics Model of PAA Hydrogel Swelling

Model	Kinetics mechanism	General expression of the kinetics model, $f(\alpha)$	Integral form of the kinetics model, $g(\alpha)$
P1	Power law	$4\alpha^{3/4}$	$\alpha^{1/4}$
P2	Power law	1	$\alpha^{1/3}$
P3	Power law	$2\alpha^{1/2}$	$\alpha^{1/2}$
P4	Power law	$2/3\alpha^{-1/2}$	$\alpha^{3/2}$
R1	Zero-order (Polanyi-Winger equation)	1	α
R2	Phase-boundary controlled reaction (contracting area, i.e., bidimensional shape)	$2(1 - \alpha)^{1/2}$	$[1 - (1 - \alpha)^{1/2}]$
R3	Phase-boundary controlled reaction (contracting volume, i.e., tridimensional shape)	$2/3$	$[1 - (1 - \alpha)^{1/3}]$
F1	First-order (Mampel)	$3(1 - \alpha)$	$-\ln(1 - \alpha)$
F2	Second-order	$(1 - \alpha)^2$	$(1 - \alpha)^{-1} - 1$
F3	Third-order	$(1 - \alpha)^3$	$0.5[(1 - \alpha)^{-2} - 1]$
A2	Avrami-Erofe'ev	$2(1 - \alpha)[- \ln(1 - \alpha)]^{1/2}$	$[- \ln(1 - \alpha)]^{1/2}$
A3	Avrami-Erofe'ev	$3(1 - \alpha)[- \ln(1 - \alpha)]^{2/3}$	$[- \ln(1 - \alpha)]^{1/3}$
A4	Avrami-Erofe'ev	$4(1 - \alpha)[- \ln(1 - \alpha)]^{3/4}$	$[- \ln(1 - \alpha)]^{1/4}$
D1	One-dimensional diffusion	$1/2\alpha$	α^2
D2	Two-dimensional diffusion (bidimensional particle shape)	$1/[- \ln(1 - \alpha)]$	$(1 - \alpha)\ln(1 - \alpha) + \alpha$
D3	Three-dimensional diffusion (tridimensional particle shape) Jander equation	$3(1 - \alpha)^{2/3}/2[1 - (1 - \alpha)^{1/3}]$	$[1 - (1 - \alpha)^{1/3}]^2$
D4	Three-dimensional diffusion (tridimensional particle shape) Ginstling-Brounshtein equation	$3/2[(1 - \alpha)^{-1/3} - 1]$	$(1 - 2\alpha/3) - (1 - \alpha)^{2/3}$

ious kinetics models together with their corresponding ranges of linearity (P) and their correlation coefficients (R).

The obtained and presented results unambiguously confirm the limited possibilities for the investigation of the kinetics of the hydrogel swelling process with the known models. This is because the kinetics curves can be described with them only at limited swelling intervals. Suggested kinetic models overcome these limitations and enable to kinetically describe the swelling process in almost the entire swelling range. Activation energies determined by that model are somewhat higher than those determined by the model of kinetics of first order chemical reactions and considerably higher than the values

determined on the basis of Fick's diffusion model. Values of the preexponential factor calculated using both the suggested model and the model of first order chemical reaction kinetics are significantly smaller than those value calculated using Fick's diffusion model.

Among the theories of the kinetics of swelling, the models of Li and Tanaka¹⁸ and Hariharan and Peppas¹⁹ are the most famous theories that are independent from the shapes of the gels. Li and Tanaka presented a theory on the swelling kinetics of gels based on the collective motions of both the network and swelling medium during the swelling process, i.e., the diffusion motion of an "adsorption complex" formed from the network and swelling medium dif-

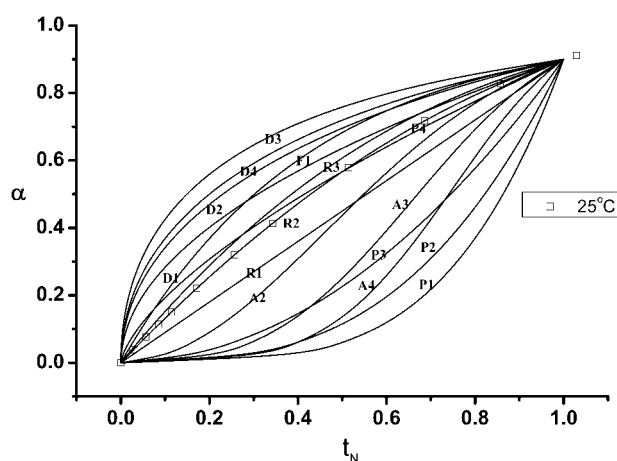


Figure 7 The plot $\alpha = f(t_N)$ for swelling in distilled water (\square) and theoretical models (solid lines).

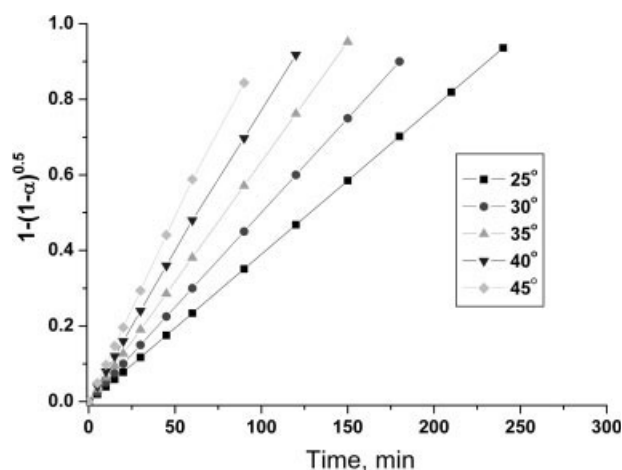


Figure 8 The plot of $1 - (1 - \alpha)^{1/2}$ versus time at investigated temperatures.

TABLE VII
The Changes of Ranges of Applicability (P), Model Swelling Rates Constants (k_m) and Correlation Coefficients (R) with Temperature

Temperature ($^{\circ}\text{C}$)	P (%)	R	k_m (min^{-1})
25	0–94	1	0.0039
30	0.90	1	0.005
35	0–95	1	0.00635
40	0–92	0.9997	0.00781
45	0–92	0.99956	0.00947

fusion. According to their theory, the swelling medium moves together with the network and the swelling medium rate is the same as the network rate. They also stated that the motion of the polymer network of a gel during the course of swelling is described by an equation known as the collective diffusion equation.²⁰ In that equation, the diffusion coefficient is defined as the ratio of the osmotic bulk modulus of the polymer network to the frictional coefficient between the polymer network and liquid.²¹

On the contrary however, Hariharan and Peppas gave the model based on the assumption that the swelling process consists of a phase transition of the gel from a glassy to a rubbery state which is described by the network's shear deformations changes during the time, under the influence of constant stress which is caused by the interaction of the molecules of the swelling medium with the polymer network.¹⁹

Equation (12) given in the present study, among the kinetics equations of the heterogeneous processes, is well known as the equation of contracting area.²² That equation was developed for the heterogeneous process taking place at the reactive interface when nucleation occurs instantaneously across the entire surface of the reagents which is of cylindrical

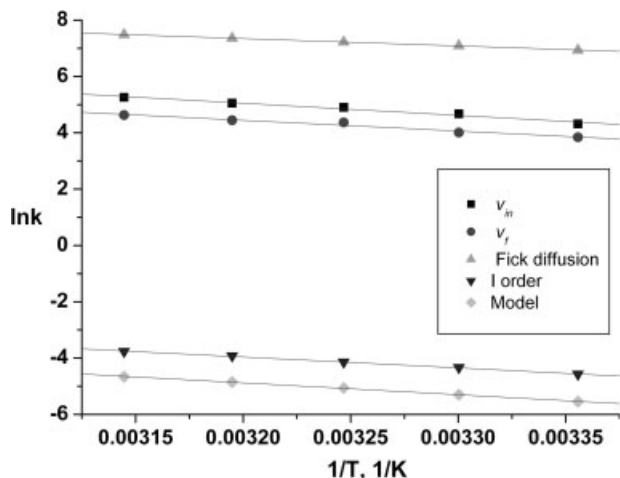


Figure 9 The $\ln k$ dependences from $1/T$ for different kinetics models.

TABLE VIII
The Kinetic's Parameters from Various Kinetic's Models

Model	P (%)	R	E_a (kJ/mol)	$\ln A$
v_{in}			35.30	18.60
v_{fin}			29.95	15.96
Fickian diffusion	22–82	0.9998	21.68	15.69
First order	0–(50–70)	0.9988	32.07	8.38
Model	0–(90–95)	0.9993	35.01	8.6

shape, i.e., expanded prism,²³ or at the ends of the particles having a disc or plate shape.²⁴

The established model of the swelling kinetics [using eq. (12)] confirms the Li and Tanaka hypothesis about diffusion motion of the "adsorption complex" formed as a result of the molecules of the swelling medium interacting with the hydrogel network, but he also makes the distinction that the so-called "collective motion" is actually just a movement of the reactive interface that is formed as a result of the interaction of the molecules of the swelling medium with the hydrogel.

Because the swelling kinetics are predetermined by both the network's elasticity and the friction of the network with the swelling medium, in the case when the elastic expansion of the network velocity is the same as the velocity of swelling medium molecules, the newly formed reactive interface has a constant value and the velocity of its movement is constant. In that case, the swelling velocity is constant (this corresponds to the initial linear part of the swelling kinetics curve) and the changes of the SDs are proportional to time. When the velocity of elastic expansion begins to decrease due to friction, the reactive interface also begins to decrease and the swelling velocity decreases until the end of the process when it is finally finished. Because of all that, eq. (12) gives a good description of the swelling process and it also presents the right kinetics model for the examined swelling process.

The activation energy for the investigated swelling process determined using the formerly mentioned model is proportional to the energy of phase transformation of the xerogel to hydrogel from a glassy to a rubbery state. This value is in agreement to that of the activation energy of the molecules of the swelling medium interacting with the hydrogel, which is furthermore in correspondence with Hariharan and Peppas' model.

CONCLUSIONS

A new model applicable for determining the kinetics model of the hydrogel swelling process was developed.

The kinetics of swelling of poly(acrylic acid) hydrogel in distilled water are determined by the

movement of the reactive interface formed between the hydrogel and water.

The activation energy of the swelling process corresponds to the energy of phase transformation of the xerogel from a glassy to a rubbery state.

References

1. Peppas, N. A.; Mikos, A. G. In *Hydrogels in Medicine and Pharmacy*; Peppas, N. A., Ed.; CRC Press: Boca Raton, 1986; Vol. 1, p 2.
2. Ratner, B. D.; Hoffman A. S. In *Hydrogels for Medical and Related Applications*; Ratner, B. D., Ed.; American Chemical Society: Washington, DC, 1976; p 1.
3. Elvira, C.; Mano, J. F.; Román, J. S.; Reis, R. L. *Biomaterials* 2002, 23, 1955.
4. Kim, S. J.; Lee, K. J.; Kim, S. I. *React Funct Polym* 2003, 55, 69.
5. Gudman, L.; Peppas, N. A. *J Appl Polym Sci* 1995, 55, 919.
6. Omidian, H.; Hashemi, S. A.; Sammes, P. G.; Meldrum, I. *Polymer* 1998, 26, 6697.
7. Katime, I.; Velada, J. L.; Novoa, R.; Diaz de Apodaca, E.; Puig, J.; Mendizabal, E. *Polym Int* 1996, 40, 281.
8. Karadağ E.; Saraydin, D. *Polym Bull* 2002, 48, 299.
9. Karadağ E.; Saraydin D.; Güven, O. *Macromol Mater Eng* 2001, 286, 34.
10. Jabbary, E.; Nazary, S. *Eur Polym J* 2000, 36, 2685.
11. Jovanovic, J.; Adnadjevic, B.; Ostojić, S.; Kićanović, M. *Mater Sci Forum* 2004, 453/454, 543.
12. Dorkoosh, F. A.; Brusse, J.; Verhoef, J. C.; Rafiee-Thrani, M.; Junginger, H. *Polymer* 2000, 41, 8213.
13. Gudeman, L. F.; Peppas, N. A. *J Appl Polym Sci* 1995, 55, 919.
14. Brown, M. E.; Dollimore, D.; Galway, A. K. *Reaction in the Solid State in Comprehensive Chemical Kinetics*; Elsevier: Amsterdam, 1980; Vol. 22.
15. Vyzovkin, S.; Wight, C. A. *Thermochim Acta* 1999, 53, 340.
16. Khawam, A.; Flanagan, D. R. *Thermochim Acta* 2005, 429, 93.
17. Hilbert, S. F. *J Br Ceram Soc* 1969, 6, 11.
18. Li, Y.; Tanaka, T. *J Chem Phys* 1990, 92, 1365.
19. Hariharan, D.; Peppas, N. A. In *Superabsorbent Polymers: Science and Technology*, ACS Symposium Series 573, Bucholz, F.; Peppas, N. A., Eds.; The American Chemical Society: Washington, DC, 1994.
20. Wang, C.; Yong, L.; Zhibing, H. *Macromolecules* 1997, 30, 4727.
21. Andersson, M.; Axelsson, A.; Zacchi, G. *J Controlled Release* 1998, 50, 273.
22. Sharp, J. H.; Brindley, G. W.; Narahari Achar, B. N. *J Am Ceram Soc* 1966, 49, 379.
23. Jacobs, P. W. M. *Mater Sci Res* 1969, 4, 37.
24. Eckhardt, R. C.; Flanagan, T. B. *Trans Faraday Soc* 1964, 60, 1289.